For L-shell vacancy, f represents the Coster-Kronig yields of the non-radiative emission process resulting vacancies in other L subshells.

This work aims to introduce data from the EADL [4] in order to evaluate the atomic database with both previous EGS4 simulation results, and previous experimental data that were measured at the KEK Photon Factory synchrotron.

2. Method

2.1 The EADL Data Library

The EADL data library is part of the DLC-179 RSIC data library, which contains the Lawrence Livermore evaluated atomic data (EADL), electron data (EEDL) and photon data libraries (EPDL). The scope of EADL is to provide atomic relaxation data for use in Monte Carlo particle transport simulation codes for Z = 1 -100. The EADL includes three main data tables: 1. Subshell data; 2. Transition probability data; 3. Whole atom data [4].

In this work, values from the transition probabilities data were extracted into the EGS5 and tabulated in the file: egs5_block_data_atom.f. The modified tables are:

1. The K and L shell fluorescence yields: ω_K, ω_1, ω_2, ω_3
2. L shell Coster-Kronig transitions: f_{12}, f_{13}, f_{23}

2.2 The Experimental Data

Several highly pure material thick targets were irradiated at the BL-14C in the KEK-PF synchrotron facility. The beamline was equipped with a monochromator to produce mono-energetic photons incident beam of 10 keV, and up to 40 keV. Two planar HPGe detectors for low-energy X-rays were set, one horizontally to the beam – target plane, and the other vertically to the plane [5]. The measurements results of the previous experiments were compared with this current study simulation results.

2.3 The Monte Carlo simulations

The Monte Carlo simulation user-code has been modified to an EGS5 user-code from the previous EGS4 version. The user-code includes a source description with specific polarization ratios versus incident photon energy. The emitted X-rays flux has been tallied with a 0.1 keV binning for each detector. 5 degrees angular aperture has been set toward each detector.

The simulation flux results are analyzed using an earlier prepared HPGE response function arrays. This procedure provides a simulated spectral response of each detector for each run. The simulation results are treated using a spectral Gaussian broadening code, in several cases where spectral results had to be compared with detector spectral measurements.

3. Results and Discussion

3.1 K-X emission

The fluorescence yields ω_K ratios of the EADL over the Table of Isotope 8th Ed., which was taken from Bambynek-1984 [10] along all elements Z number are plotted in Fig. 1. Three targets used in this study were Fe, Cu and Ti, and their location is shown in Fig. 1, which allows us to predict a difference in their calculations results.

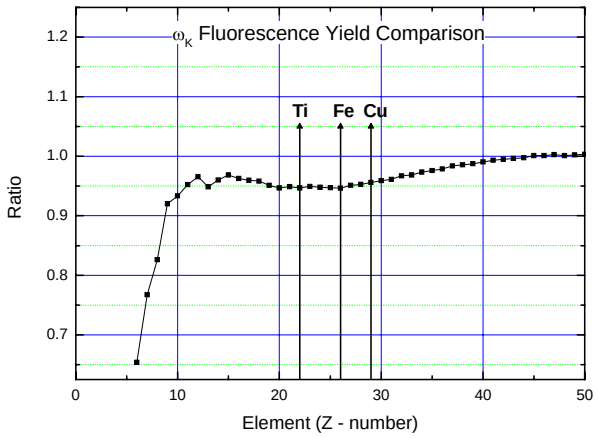

Figure 1: The fluorescence yields ω_K ratios of the EADL over the Bambynek 1984 yields. The tested targets are shown as arrows.

The K-X emissions of these materials were measured in high performance of spectral resolution and counts. Total K fluorescence counts measured-over-calculated ratios are shown versus the incident photon beam energy. In Fig. 2 the simulations results were obtained using the Bambynek 1984 fluorescence values taken from The Table of Isotopes - 8th edition. The results of the horizontal detector (H) and the vertical detector (V) ratios were averaged for each point. The results of K fluorescence counts measured-over-calculated ratios using the EADL data are shown in Fig. 3. The pulse-height distributions of each detector from the Monte Carlo simulations results and the measurements on iron target are shown in Fig. 4.
The M/C ratios showed an improved agreement for all the K-X emission results, and the EGS5 spectral results present very good agreement with the measured spectra in both detectors.

3.2 L-X emission

The total L-X peak counts were compared to the M/C counts ratios for three targets: Gd, W and Pb, as shown in Fig 5. Also the individual L emissions, Lα, Lβ and Lγ emission peaks, were compared to the experimental results, in Fig.6.
The Lα, Lβ and Lγ emission peaks M/C results, using the EADL data, are presented in Fig. 7. From Fig.6 and Fig. 7, we found that the Lβ and Lγ M/C ratios in Gd were improved with the EADL data, however the Lα M/C ratio diverge away. A similar trend is observed in lead. The tungsten results show this discrepancy for all the emission peaks M/C ratios. The explanations how the EADL data led to the L emissions mismatch are described in section 3.3.

In order to test Campbell (2003) recommendations, we modified again the fluorescence yields and Coster-Kronig yields due to Campbell data [7]. The resulted total L-emissions, and the Lα, Lβ and Lγ emission peaks were compared to the experimental results for each case, as shown in Fig. 8, and in Fig. 9.
The Campbell recommended database led to the closest agreement in most of the cases for the Lα, Lβ and Lγ emission peaks.

3.2 Investigation of the Coster-Kronig yields and energies

[9] T.Papp, "On the accuracy of L subshell ionization cross sections: II. Coster-Kronig transition probabilities", ATOMKI, Annual Report, 37, Institute of Nuclear Research of the Hungarian Academy of Sciences, Debrecen, Hungary (2005).
[10] W. Bambynek, post-deadline abstract in the Proceedings of the Conference on X-ray and Inner shell Processes in Atoms, Molecules and Solids, Leipzig, Aug 20-24 (1984).

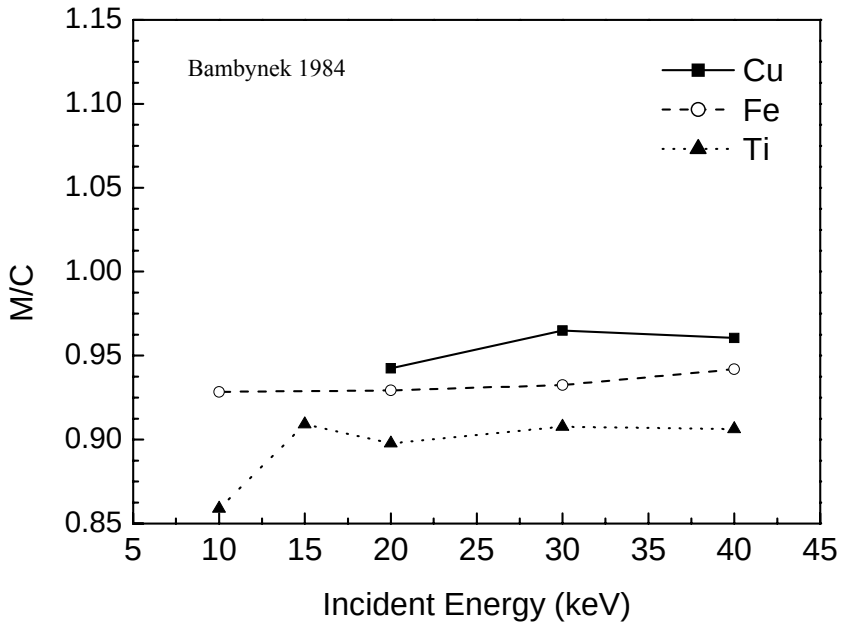

Figure 2: The K – X emission Measured/Calculated ratios in Cu, Fe and Ti using the Bambynek 1984 database.

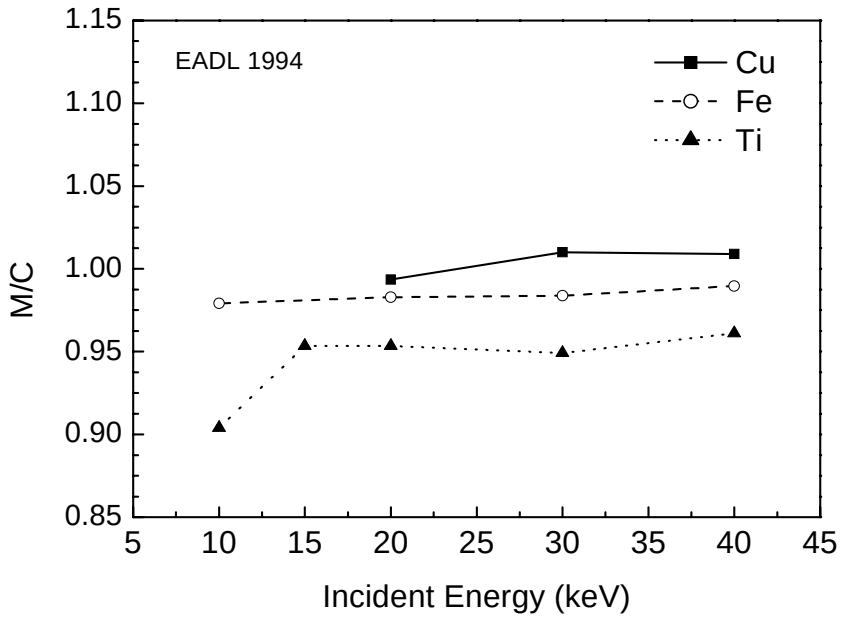

Figure 3: The K – X emission Measured/Calculated ratios in Cu, Fe and Ti using the EADL 1994 database.

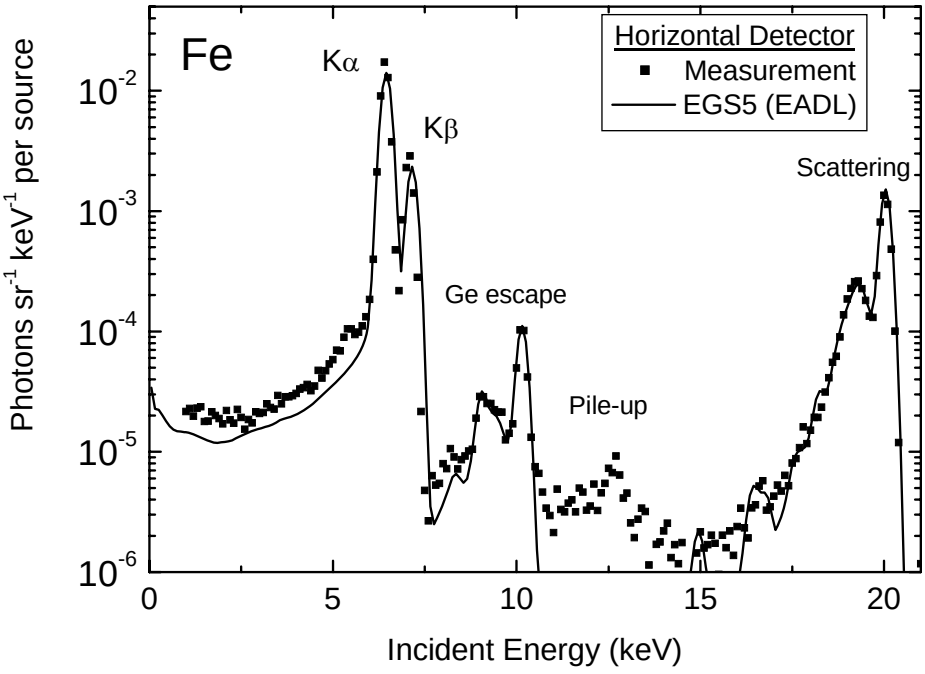

Figure 4: Spectrum comparison of the K – X lines of iron target for the horizontal detector. The calculated results were obtained using the EADL K fluorescence yields.

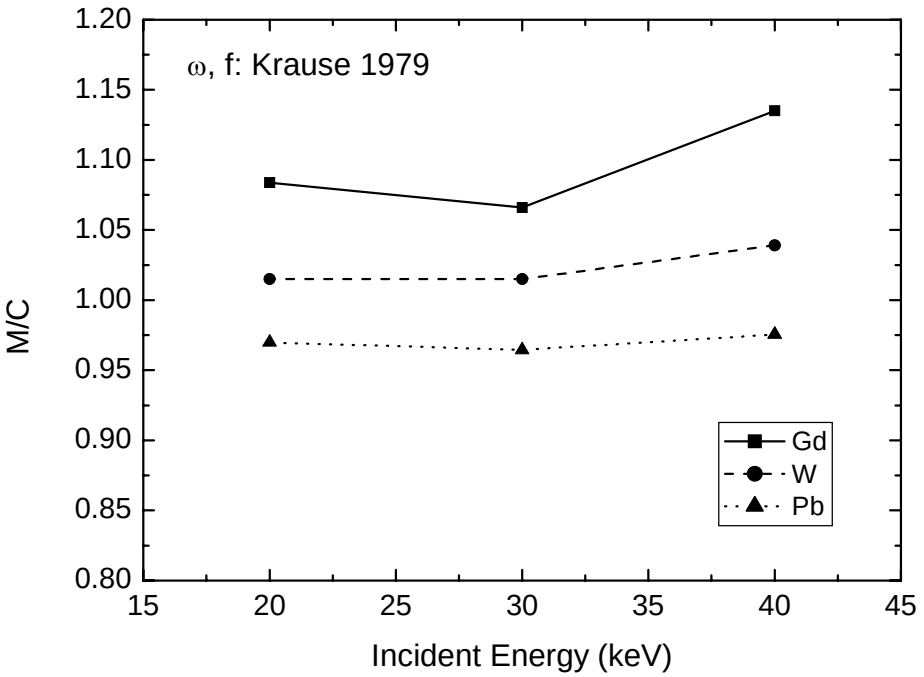

Figure 5: The Measured over Calculated total L – X emission counts ratios in gadolinium, tungsten and lead using the Krause 1979 yields, which was adopted in Table of Isotope 8th edition.